Experimental Neurology 218 (2009) 24–32

Contents lists available at ScienceDirect

Experimental Neurology

journal homepage: www.elsevier.com/locate/yexnr

Conditional inactivation of the *NBS1* gene in the mouse central nervous system leads to neurodegeneration and disorganization of the visual system

Koby Baranes [a,1], Dorit Raz-Prag [a,1], Anat Nitzan [a,b], Ronit Galron [a], Ruth Ashery-Padan [c], Ygal Rotenstreich [b], Yaniv Assaf [b], Yosef Shiloh [c], Zhao-Qi Wang [d,e], Ari Barzilai [a], Arieh S. Solomon [b,*]

[a] *Department of Neurobiology, George S. Wise Faculty of Life Sciences, Tel Aviv University, Tel Aviv, 69978 Israel*
[b] *Goldschleger Eye Research Institute, Tel Aviv University, Sheba Medical Center, Tel Hashomer, 52621, Israel*
[c] *Department of Human Molecular Genetics and Biochemistry, Sackler School of Medicine, Tel Aviv University, Tel Aviv, 69978 Israel*
[d] *Lebnitz Institute for Age Research-Fritz Lipman Institute e.V., Germany*
[e] *Faculty of Biology and Pharmacy, Friedrich-Schiller University Jena, 07745 Jena, Germany*

ARTICLE INFO

Article history:
Received 13 August 2008
Revised 15 February 2009
Accepted 19 March 2009
Available online 1 April 2009

Keywords:
Nijmegen breakage syndrome (NBS)
Ataxia telangiectasia (A-T)
MRI
Nbs1
White matter
Myelin
Oligodentrocytes

ABSTRACT

Nijmegen breakage syndrome (NBS) is a genomic instability disease caused by hypomorphic mutations in the *NBS1* gene encoding the Nbs1 (nibrin) protein. Nbs1 is a component of the Mre11/Rad50/Nbs1 (MRN) complex that acts as a sensor of double strand breaks (DSBs) in the DNA and is critical for proper activation of the broad cellular response to DSBs. Conditional disruption of the murine ortholog of the human *NBS1*, Nbs1, in the CNS of mice was previously reported to cause microcephaly, severe cerebellar atrophy and ataxia. Here we report that conditional targeted disruption of the murine *NBS1* gene in the CNS results in mal-development, degeneration, disorganization and dysfunction of the murine visual system, especially in the optic nerve. Nbs1 deletion resulted in reduced diameters of Nbs1-CNS-Δ eye and optic nerve. MRI analysis revealed defective white matter development and organization. Nbs1 inactivation altered the morphology and organization of the glial cells. Interestingly, at the age of two-month-old the levels of the axonal guidance molecule semaphorin-3A and its receptor neuropilin-1 were up-regulated in the retina of the mutant mice, a typical injury response. Electroretinogram analysis revealed marked reduction in a- and b-waves, indicative of decreased retinal function. Our study points to a novel role for Nbs1 in the development, organization and function of the visual system.

Introduction

Nijmegen Breakage Syndrome (NBS) is a rare autosomal recessive disorder characterized by microcephaly, mental deficiency, "bird-shaped" face, immunodeficiency, predisposition to lymphoreticular malignancies, chromosomal instability, and radiation sensitivity (Chrzanowska et al., 1995; Digweed and Sperling, 2004; Seemanova et al., 1985; van der Burgt et al., 1996; Weemaes et al., 1981). NBS is caused by hypomorphic mutations in the *NBS1* gene, which encodes the Nbs1 (nibrin) protein (Carney et al., 1998; Varon et al., 1998). Nbs1, together with the Mre11 and Rad50 proteins, constitute the NRM complex, a sensor of double strand breaks (DSBs) in the DNA (Carney et al., 1998; Stracker et al., 2004). The MRN complex is required for proper initiation of the DNA damage response to DSBs.

Nbs1 exerts its biological activities as part of the extensively documented sensor, the MRN complex. This complex is rapidly recruited to DSB sites where it tethers and processes the broken ends (Lavin, 2007; Lukas and Bartek, 2004; Moreno-Herrero et al., 2005; Stracker et al., 2004). In concert with Ataxia telangiectasia mutated (ATM), Ataxia telangiectasia and Rad3-related (ATR), MDC1 and H2AX [4], the MRN complex activates an intricate web of signals that facilitate DNA repair.

Knocking out the murine homolog of *NBS* (*Nbs1*) led to embryonic lethality (Dumon-Jones et al., 2003; Frappart et al., 2005; Zhu et al., 2001). Heterozygous animals ($Nbs1^{+/-}$) developed malignant tumors and were sensitive to ionizing radiation (Dumon-Jones et al., 2003). When *Nbs1* was conditionally inactivated in the central nervous system (CNS) by the nestin-Cre conditional gene targeting system (Frappart et al., 2005), the animals (Nbs1-CNS-Δ) showed micro-cephaly, cerebellar mal-development and ataxia. These abnormalities are reminiscent of the clinical presentation of NBS and of advanced ataxia telangiectasia (A-T). Thus, Nbs1-CNS-Δ mice represent a chromosomal instability disorder that resembles both these diseases. In our previous study we have found that Nbs1 deletion led to cerebellar disorganization and markedly hampered the development and organization of the white matter (Assaf et al., 2008). Using Nbs1-CNS-Δ mice, Yang et al. (2006) reported that deletion of Nbs1 in mice

* Corresponding author. Fax: +972 3 5351577.
E-mail address: asolomon@post.tau.ac.il (A.S. Solomon).
[1] Contributed equally to the paper.

0014-4886/$ – see front matter © 2009 Elsevier Inc. All rights reserved.
doi:10.1016/j.expneurol.2009.03.026

causes microphthalmia and cataract due to reduced proliferation of the lens epithelial cells and altered lens fiber cell differentiation. This result implies a novel function of Nbs1 in lens development.

Semaphorins comprise a large family of secreted and membrane-associated proteins that can signal axon repulsion and/or attraction (reviewed in Van Vactor and Lorenz, 1999). Semaphroin-3A acts as a repulsive cue in axonal pathway formation during neuronal development (Luo et al., 1995; Messersmith et al., 1995). In addition to its repulsive activity, sema3A is capable of inducing apoptosis of various types of neuronal cells (Gagliardini and Fankhauser, 1999; Shirvan et al., 2002; Shirvan et al., 1999). Sema3 proteins convey their signals through the activation of a neuronal receptor complex that contains neuropilins (NPs) and plexins as ligand binding and signal transducing subunits, respectively (Raper, 2000).

In the present work, conditional deletion of Nbs1 in the CNS slightly hampered the normal development of the mutant mouse visual system but caused severe degeneration of retinal ganglion cells and the optic nerve. MRI analysis of the Nbs1-CNS-Δ mice revealed reduced eye and optic nerve size as well as significant myelin damage. Light microscopy analysis disclosed altered expression of astrocytes and oligodendrocytes in these mice. Remarkably, the levels of Sema3A and NP1 were up-regulated in retinas of mutant mice. The electroretinogram (ERG) of the Nbs1-CNS-Δ mice was significantly diminished, indicative of retinal dysfunction. Collectively, our data point to the importance of a proper DNA damage response (DDR) to the development, organization and function of the visual system.

Methods and materials

Tissue preparation

Tissues (isolated retinas and optic nerves) were dissected from 8 to 12-week-old male Nbs1-CNS-Δ and age-matched Nbs1-CNS-ctrl littermates. The retinas and optic nerves were isolated and fixed in 4% paraformaldehyde (Merck, Darmstadt, Germany) in phosphate buffer saline (PBS) for 1–2 h, then infiltrated for cryo-protection with 4% sucrose (Merck) at 4 °C for 2 h, followed by 20% sucrose plus 5% glycerol (Merck) in PBS overnight at the same temperature. Fixed tissue was embedded in Tissue Freezing Medium (Leica Instruments GmbH, Nussloch, Germany) and quickly frozen in liquid nitrogen. Cross-sections (10 μm) were placed on subbed slides (0.5% gelatin, containing 0.05% chromium potassium sulfate) and stored at 20 °C.

MRI analysis

MRI was carried out with 1% isoflurane (Abbott, England) in 95% oxygen anesthesia for 30 min. During the MRI scan, mouse body temperature was kept at 37 °C using a blanket of warm water circulation, and respiration was kept around 30 breath cycles per minute. The protocol was approved by the Tel Aviv University Committee for Experiments in Animals. The two groups of mice (Nbs1-CNS-Δ and Nbs1-CNS-ctrl) were scanned in a 7T/30 spectrometer (Bruker, Germany) using a 10 mm surface coil and 400 mT/m gradient system.

Image analysis

The multi-echo T_2 weighted images were used to generate quantitative T_2 maps. The multi-echo signal was fitted to a mono-exponential decay function on a pixel-by-pixel basis to extract the T_2 value for each image pixel. The DWI-EPI data was analyzed using the diffusion tensor imaging (DTI) analysis system (Basser and Pierpaoli, 1998; Pierpaoli and Basser, 1996; Pierpaoli et al., 1996) to produce the fractional anisotropy (FA), apparent diffusion coefficient maps (ADC), parallel diffusivity ($D_{\|}$), and radial diffusivity ($D_{\perp}$). While ADC maps show an iso-intense signal in both gray matter and white matter, the FA maps are more specific to white matter and have a relatively high signal in white matter regions.

Western blot analysis

Western blot analysis was performed as described by Harlow and Lane using 10% polyacrylamide gels. Each lane was loaded with an equal amount of protein extracts, which, following electrophoresis, were transferred to an immobilon polyvinylidene disulfide (PVDF) membrane (Millipore, Billerica, MA) for 1.5 h. Blots were stained with Ponceau to verify equal loading and transfer of proteins, and incubated with 5% low-fat milk in buffer TBST (Tris 20 mM, NaCl 150 mM, 1% Tween 20, Sigma) for 1 h. Membranes were then probed with polyclonal Nbs1 (p95) antibody (abcam-ab23996, Cambridge UK) (1:1000, washed three times with 5% low-fat milk in TBST, and incubated with anti-rabbit IRDye 800CW secondary antibody (1:10,000; LI-COR, Lincoln, NE). The intensity of the signal was determined using the Odyssey infrared imaging system (LI-COR, Lincoln, NE).

Quantitative RT-PCR analysis

Two retinas from each animal were pooled and subjected to RNA extraction using MasterPure RNA Purification kit (Tamar MCR85102). Total RNA concentration was determined with nanodrop analysis assay (260/280 nm) and the purity of the extraction was further determined (240/260 nm>1.9). The total RNA concentration was diluted with molecular water (DNase, RNase free) (Sigma W4502) to achieve 500 ng, which was later converted into cDNA using Verso cDNA kit. The quantification of *NBS1* mRNA expression was conducted via reverse transcription followed by quantitative real-time polymerase chain reaction (QRT-PCR) using TaqMan (Absolute Blue QPCR ROX Mix, Tamar AB-4138). Reverse transcriptase PCR assays were designed by Applied Biosystems (Carsland, CA) and compared with β-actin (ACTB) RNA levels. The comparative Ct method was used for quantification of transcripts according to the manufacturer's protocol. The primers used were: Nbs1 MM01210905M1 (Applied Biosystem, Carsland, CA). Measurement of ΔCt was performed in duplicates or triplicates. All reactions were performed with primer concentration of 0.25 μM in a total volume of 10 μl reaction.

Retrograde labeling of RGC

Retrograde labeling of RGC was carried out using the lipophilic neurotracer dye 4-(4-(didecylamino) styryl)-N-methylpyridinium iodide (4-Di-10-Asp; Molecular Probes, Inc.) as previously described (Lazarov-Spiegler et al., 1999; Shirvan et al., 2002).

Electron microscopy

Optic nerves from the two genotypes were dissected out and fixed in 4% gluteraldehyde in 0.1 M cacodilate buffer (pH-7.4). After fixation, 100 μm blocks were cut from the various regions of the optic nerve (near the eye globe and close to the optic chiasm). The blocks were rinsed in cacodilate buffer, post-fixed in 1% OsO_4 in PBS, and washed again. After dehydration in graded ethanol solution, the tissues were embedded in glycid ether 100 (Serva, Heidelberg, Germany). Ultra-thin sections (~0.1 μm) were stained with uranyl acetate and led citrate and examined in Jeol 1200 EX TEM (Jeol, Tokyo, Japan). We chose the middle of the optic nerve, which is rich in axons and enables measurement of the myelin index.

Immunocytochemical analysis

Immunohistochemical analysis was performed on frozen sections of retina and optic nerve from WT and Nbs1-CNS-Δ mice as described in Shirvan et al. (2002).

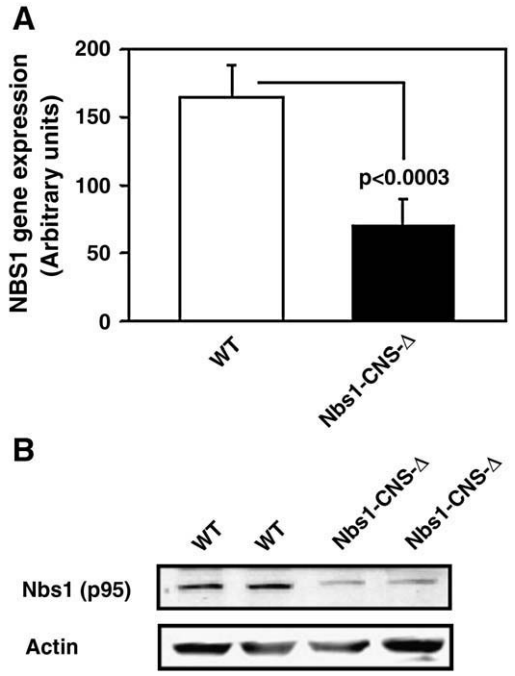

Fig. 1. Reduced expression of Nbs1 in Nbs1-CNS-Δ mice. (A) Reduction in Nbs1 gene expression in the retina vs. housekeeping gene actin in Nbs1-CNS-Δ mice as evident by quantitative RT-PCR analysis. (B) Western blot analysis displaying a significant reduction in the Nbs1 protein in the retina ($n=4$, $p<0.05$).

Confocal imaging was performed using a Zeiss LSM 510 microscope. Some sections were incubated with pre-immune serum as control. Slides stained for microglia were incubated with isolectin-B4 (IB4) (1:100; Vector, Peterborough, UK) in a buffer containing PBS, $CaCl_2$ (0.1 mM; Merck), $MgCl_2$ (0.1 mM; Merck), and Triton X-100 (0.1%; Sigma), without blocking, for 5 h at room temperature, followed by overnight incubation at 4 °C. Sections were then washed, stained with Sytox blue, washed again with the same buffer and mounted with aqueous mounting medium.

Electroretinogram (ERG) recording

Animals were prepared under dim red light following a minimum of 7 h dark-adaptation. Anesthesia was induced by intraperitoneal injection of ketamine (80 mg/kg) and xylazine (4 mg/kg), and body temperature was maintained with a heating pad. Electroretinographic responses (ERGs) were recorded after fully dilating the pupils with topical corneal 0.5% tropicamide and 2.5% phenylephrine HCl. A gold-wire loop electrode was placed on the cornea after topical 0.5% proparacaine HCl anesthesia. A gold-wire reference electrode was positioned to touch the sclera near the limbus of the eye, and a neutral electrode was clipped to the ear. ERGs were recorded with the LKC system (LKC Technologies, Gaithersburg, MD) with a hand-held mini-ganzfeld. Dark-adapted responses were recorded across a 5 log unit range of stimulus intensity in 1 log unit steps up to maximum intensity of 1.4 log cd s/m^2. Light-adapted responses were recorded against a constant white background light of 30 cd/m^2 that suppresses rod function. ERG responses were amplified and filtered (0.3–500 Hz).

Results

mRNA and protein levels of Nbs1

To examine Nbs1 expression in the retina we used both RT-PCR and western blot analyses. In the Nbs1-CNS-Δ retinas, a significant reduction of 60% ($n=5$, $p<0.0003$ in Student's *t*-test) of Nbs1 mRNA was observed (Fig. 1A) implying that the Cre recombinase results in effective downregulation of the *NBS1* gene in the retina. Western blot analysis revealed 75% ($n=4$, $p<0.05$) reduction in the expression levels of the Nbs1 protein (Fig. 1B).

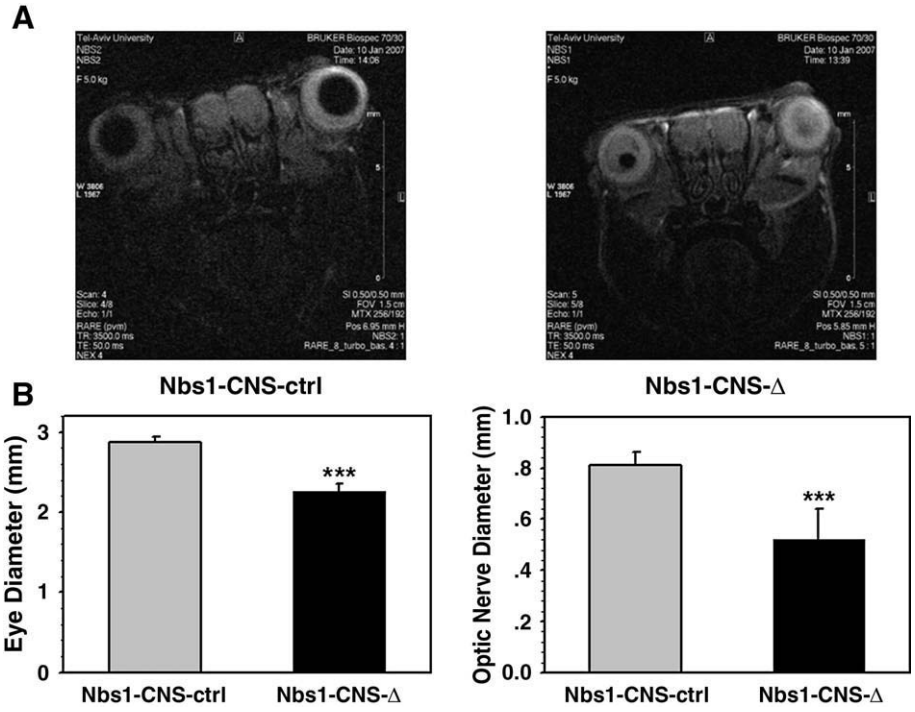

Fig. 2. Images of Images of T_2 maps: (A) Representative coronal T_2-weighted map of Nbs1-CNS-ctrl (left) and Nbs1-CNS-Δ (right) mice. Note the major differences in the opacity of the lens of the Nbs1-CNS-Δ mice. (B) Following MRI analyses, the diameters of the eyes and the optic nerves (before their conversion into the chiasm) of the two groups were measured. Note that Nbs1 deletion significantly reduced the diameter of both the eye and the optic nerve. $n=9$, *** = $p<0.0001$.

MRI

T_2 weighted MRI revealed significant morphological and contrast changes between the Nbs1-CNS-Δ and Nbs1-CNS-ctrl visual systems. The diameters of the eyes and optic nerves of the Nbs1-CNS-Δ mice were significantly smaller than those of the Nbs1-CNS-ctrl mice (Fig. 2). These qualitative observations were quantified by calculating the T_2 values in each image voxel, followed by ROI analysis with special emphasis on the optic nerve (Fig. 2B). In addition, the T_2-weighted image of the Nbs1-CNS-ctrl lens appeared as a black (low signal) round area in the center of the eye while the mutant lens appeared white (high signal). These T_2 changes indicate a more fluid composition of the content of the mutant lens compared to the control lens (Fig. 2). T_2 maps (Fig. 3) showed diffuse changes across the brain (just before the optic chiasm), most pronounced in the corpus callosum and the optic nerve.

The reduced diameter of the optic nerve may result from a reduced number of RGC axons, decreased intra-optic nerve organization, or damage to the white matter. To examine the nature of the white matter changes in the visual system of the Nbs1-CNS-Δ a DTI protocol was used. This advanced MRI application, which provides unique and more specific information on white matter (Basser and Pierpaoli, 1998; Pierpaoli and Basser, 1996; Pierpaoli et al., 1996), extracts 4 indices: FA, parallel and radial diffusivities (in relation to white matter fiber axis, i.e. parallel and perpendicular to the neuronal fibers), and ADC. DTI analysis revealed widespread white matter damage in the optic nerve (Table 1). Significant reduction in FA values was mainly due to increased radial diffusivity (Table 1). Radial diffusivity was the most sensitive parameter, with a 43% increase.

Electroretinogram (ERG)

Retinal function was evaluated by ERG. In dark adapted responses of mature mice, b-wave amplitudes of the Nbs1-CNS-Δ were significantly lower than that of the control Nbs-CNS-ctrl mice across the range of stimulus intensities (Fig. 4). Amplitudes of the a-wave showed a similar trend. Similarly, b-wave amplitudes of the light adapted responses were lower in the Nbs-CNS-Δ than in the responses of the control mice, though values were not statistically significant. To assess if these differences result from a degenerative process or a developmental one, we also examined retinal function in younger mice of 1 month age, at which the retina completes its development. B-wave amplitudes of the dark adapted responses were consistently 40% lower in the responses of the 1-month-old Nbs-CNS-Δ relative to the control (average and standard error at highest stimulus intensity were 300 ± 84 μV, $n = 6$, in the Nbs-CNS-Δ versus 496 ± 88 μV, $n = 6$ in the control mice) however differences were not statistically significant Supplementary data, (Fig. S1).

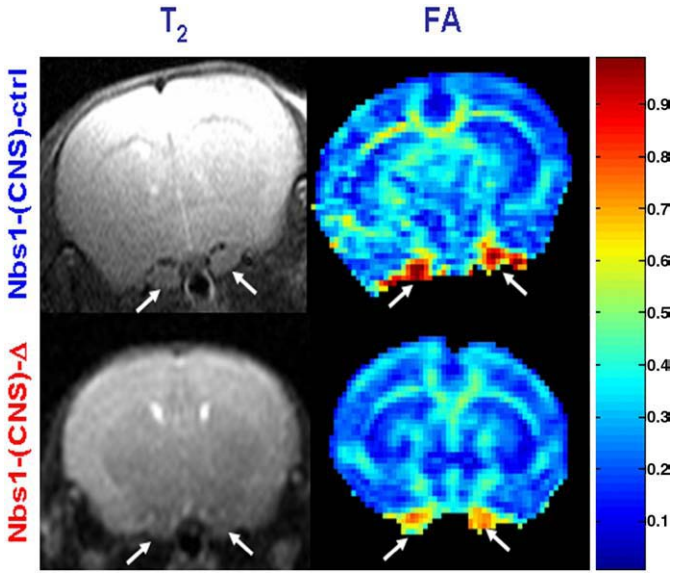

Fig. 3. Quantitative T_2 analysis: T_2 maps in coronal orientations of Nbs1-(CNS)-ctrl mice (upper images) and Nbs1-CNS-Δ mice (lower images). The color-scale represents the T_2 values in ms as indicated on the color bar at the right. Arrows point to regions of the optic nerve. The sections were taken just before the optic chiasm.

Table 1
Optic nerve analyses by DTI of T_2 maps, fractional anisotropy (FA), apparent diffusivity coefficient (ADC), and radial diffusivity $D_\perp$ of the white matter in Nbs1-CNS-ctrl and Nbs1-CNS-Δ mice.

Index	Nbs1-CNS-ctrl	Nbs1-CNS-Δ	Student *t*-test, *p* value
FA	0.75 ± 0.04	0.62 ± 0.05	<0.005
ADC[a]	0.90 ± 0.07	0.90 ± 0.06	n.s.
$D_{\|}$[a]	1.89 ± 0.20	1.62 ± 0.07	<0.05
$D_\perp$[a]	0.30 ± 0.05	0.43 ± 0.08	<0.02

Values represent average ± standard deviation, $N = 9$.
[a] ADC, $D_{\|}$ and $D_\perp$ in units of $\times 10^{-3}$ mm^2/s.

Morphology

To further study the neurological effect of Nbs1 CNS conditional inactivation, we analyzed age-dependent morphological and biochemical alterations in Nbs1-CNS-Δ lens, retina and optic nerve. Examination of the Nbs1-CNS-Δ mice revealed that all the adult animals exhibited *leukochoria* (white pupil) (Supplementary data, Fig. S2). Bilateral opacity (cataract) was evident in all Nbs1-CNS-Δ mice lenses between 8 and 12 weeks of age. The cataract was formed in the center of the lens (Supplementary data, Fig. S2). No cataract was observed in Nbs1-CNS-ctrl littermates. The lenses isolated from adult Nbs1-CNS-Δ were less rigid than those of Nbs1-CNS-ctrl mice. These results are compatible with the recent report of Yang et al. (2006). Morphological analysis of the whole eye revealed that CNS Nbs1 inactivation led to subtle changes in retinal structure. Age-dependent examination revealed a significant increase in Nbs1-CNS-Δ width in newborn as well as 2-month-old retina (between 18 and 24%, $p < 0.05$ at the age of two months). Interestingly, no marked alterations were detected in the structure of the Nbs1 mutant layers (Supplementary data, Fig. S3).

To assess the condition of the Nbs1 mutant RGC, WT and mutant retinas were labeled with the retrograde tracer Di-Asp. Only RGC that have axons capable of transporting the dye are labeled using this method. Fig. 5 shows numerous labeled RGCs in WT retinas, whereas no labeled RGC were observed in Nbs1-CNS-Δ retinas. These results do not imply that all of the Nbs1-CNS-Δ RGC are not viable as it is possible that the internal axonal transport machinery failed to transfer the dye toward the RGC body in the living cells. These results prompted us to visualize the change at the level of the Nbs1-CNS-Δ RGC axons. For this purpose we subjected optic nerve samples from Nbs1-CNS-ctrl and Nbs1-CNS-Δ mice to confocal and electron microscopy (EM). Marked reduction in white matter was evident in Nbs1-deficient optic nerves (Figs. 6A and B). EM analysis showed that the Nbs1-CNS-ctrl mice showed the typical ordered arrangements of packed axons (Fig. 6C) thickly wrapped by myelin. In contrast, the Nbs1-CNS-Δ mice showed fewer underdeveloped, loosely packed axons wrapped with thin layers of myelin (Fig. 6D). This reflects immature and underdeveloped or degenerated optic nerve. Analysis of the myelin index (thickness of the axon outer diameter divided by its inner diameter) showed a significant reduction of 54% in the Nbs1-CNS-Δ optic nerve compared to Nbs1-CNS-ctrl (Fig. 6E). Further optic nerve analysis disclosed that CNS Nbs1 inactivation caused optic nerve disorganization, a finding supported by the morphology of the extracellular matrix (ECM). Anti-fibronectin antibody was used to analyze

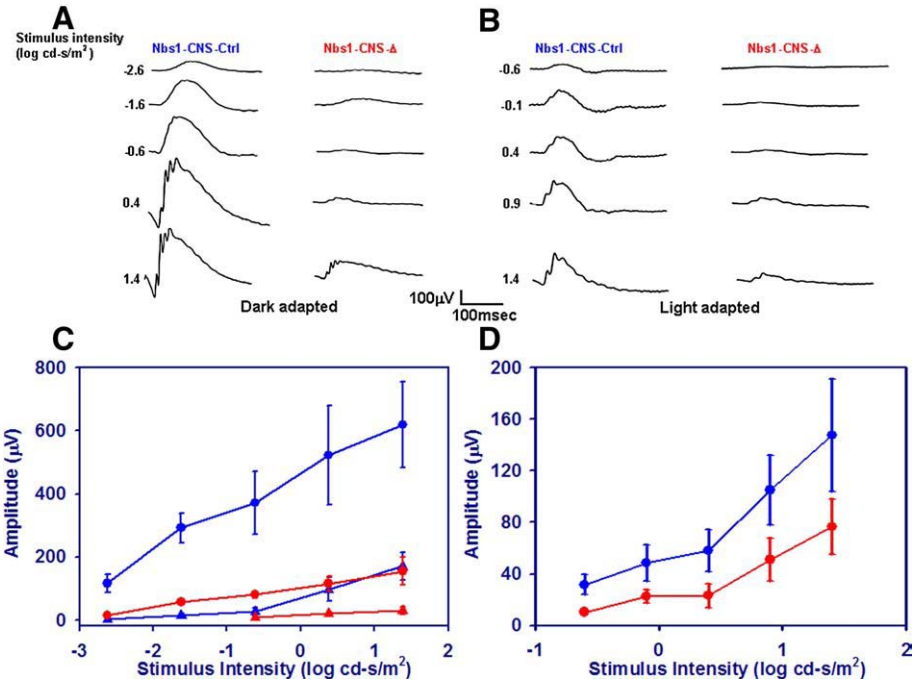

Fig. 4. ERG analysis of ERG analysis of Nbs1-(CNS)-ctrl and Nbs1-CNS-Δ mice. Representative waveforms of dark- (A) and light- (B) adapted flash ERG responses of 7–10 months old Nbs1-CNS-ctrl and Nbs1-CNS-Δ mice. (C) The a-wave (triangles) and b-wave (circles) intensity-response curves of the dark-adapted ERGs of Nbs1-CNS-Δ ($n=3$, red) and age-matched Nbs1-CNS-ctrl ($n=5$, blue) mice. Averages and standard error bars are shown. The b-wave amplitudes were significantly different between the groups (Student's *t*-test, $p \leq 0.05$). (D) Intensity-response curve of b-wave amplitudes in light adapted responses.

alterations in the organization of the ECM in the optic nerves of the two genotypes. Whereas at birth fibronectin molecules generated an organized fibrillar network-like structure in both genotypes, there was a marked increase in fibronectin immunoreactivity and loss of intra-optic nerve organization in 2-month-old Nbs1-CNS-Δ optic nerve (Supplementary data, Fig. S4).

Our results thus far indicated that *Nbs1* inactivation caused RGC functional loss and markedly altered optic nerve morphology. To further analyze the molecular and cellular mechanisms that underlie these apparent alterations, we examined the expression of sema3A and its receptor NP-1. In previous studies we found that Sema3A was up-regulated in the visual system (retina and optic nerve) in response to axotomy (Shirvan et al., 2002), glaucoma (Solomon et al., 2003) and retinal detachment (Kelbanov et al., 2009). Whereas at age 2 months the expression level of sema3A was up-regulated in Nbs1-CNS-Δ retinas as well as optic nerves (Fig. 7), no alterations in Sema3A levels were detected in 1-day-old Nbs1 deficient retina (Supplementary data, Fig. S5). Similar results were observed for NP-1 expression. An age-dependent increase in NP-1 expression in Nbs1 mutant retinas was observed (Fig. 7). To examine whether increased expression of sema-3A is associated with apoptosis, we measured the levels of phospho-p38 and JNK. Western blot analysis revealed no alterations in phospho-p38 or JNK levels in Nbs1-CNS-Δ retinas. No alterations of NP-1 were detected in 1-day-old mutant retinas (Supplementary data, Fig. S6). Collectively, these results suggest Nbs1-deletion generates conditions that resemble either retinal or optic nerve injuries rather than severely affect retinal and optic nerve development.

To analyze the effect of Nbs1 inactivation on the morphology and organization of glial cells, we immunoreacted retinas and optic nerves with GFAP (a marker of Muller cells and astrocytes) and GalC (a marker of mature oligodentrocytes). No differences in GFAP labeling were detected in 1-day-old and 2-month-old Nbs1-CNS-Δ and Nbs1-CNS-ctrl retinas. (Fig. 8, left panel and Supplementary data, Fig. S7). In Nbs1-CNS-Δ optic nerves there was increased GFAP labeling which indicated an elevated number of astrocytes compared to their Nbs1-CNS-ctrl littermates.

To further analyze the level of organization of the optic nerve as a function of Nbs1 expression, we traced the organization of

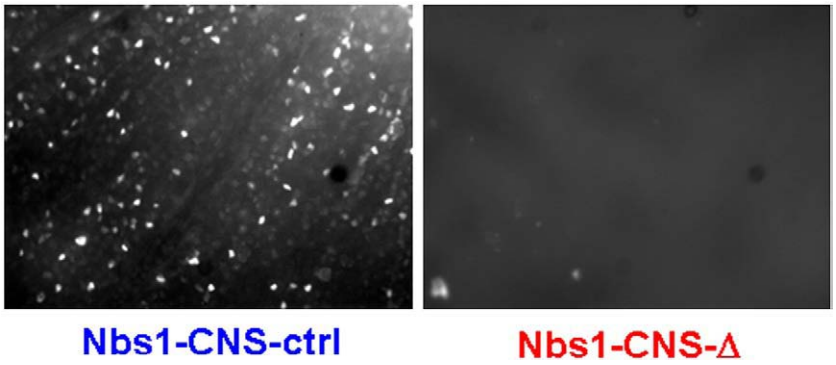

Fig. 5. Abolishment of RGCs labeling in Nbs1-CNS-Abolishment of RGCs labeling in Nbs1-CNS-Δ retinas. Whole mounted retinas in which the ganglion cells were retrogradely labeled with the neurotracer dye 4-Di-10-Asp. Representative micrographs corresponding to the median retinal areas are shown. Note that virtually all RGCs labeling was abolished in Nbs-CNS-Δ mice.

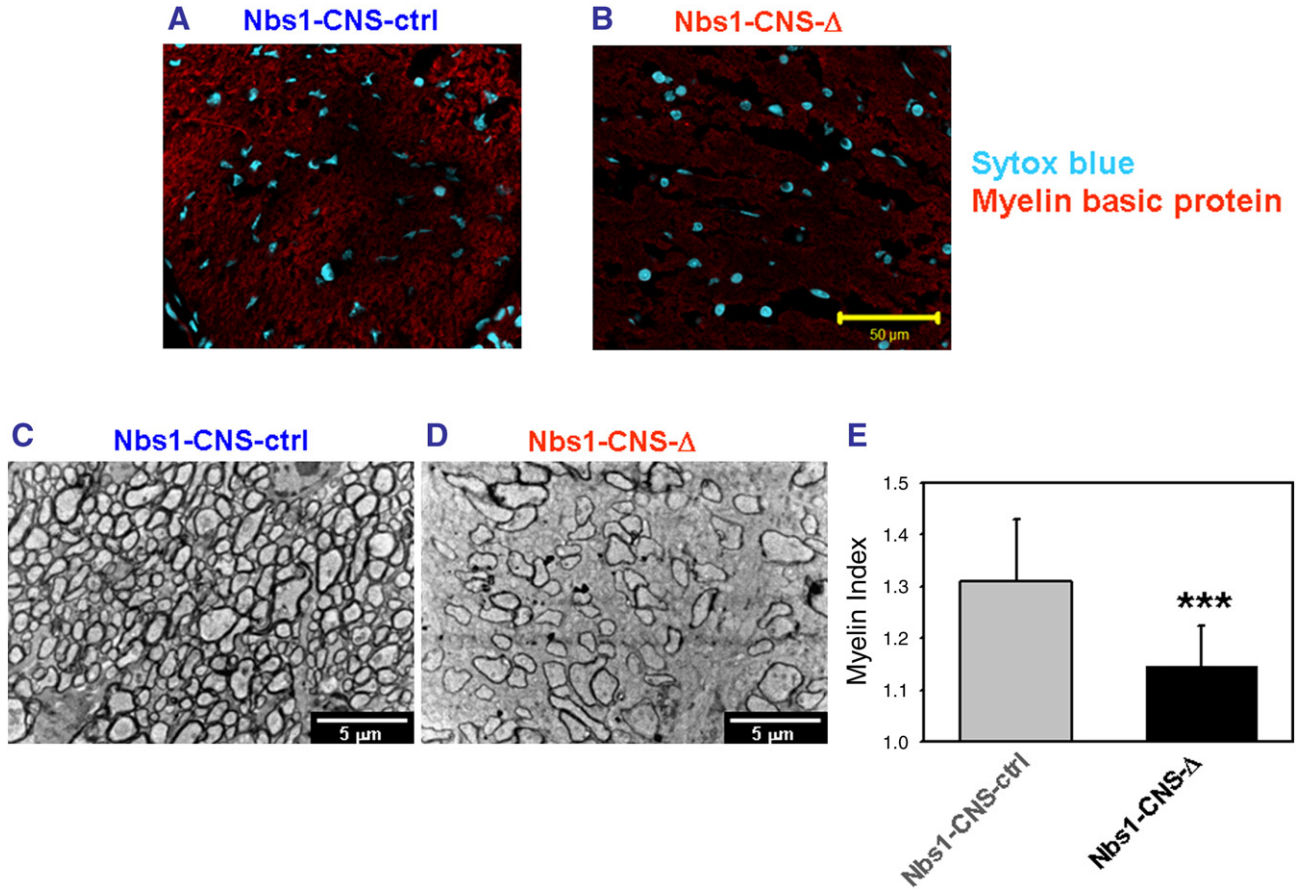

Fig.. 6 Morphological appearance of axons in Nbs1-CNS- Morphological appearance of axons in Nbs1-CNS-Δ and Nbs1-CNS-ctrl: Confocal microscopy of 2-month-old Nbs1-CNS-ctrl mouse (A) and Nbs1-CNS-Δ mouse (B) stained with anti-myelin basic protein-antibody. Electron microscopy section (coronal) through the optic nerve of 2-month-old Nbs1-CNS-ctrl mouse (C) and Nbs1-CNS-Δ mouse (D) showing underdeveloped axons and reduced myelin thickness in the latter, reflecting immature optic nerve. (E) Myelin index analysis (outer diameter divided by the inner diameter), in which Nbs1-CNS-Δ mice show values closer to 1, indicating a hypomyelination pathology. $^{**}p<0.005$. $N=3$.

oligodentrocyte cells. Nbs1-deletion disrupts the organization of oligodentrocytes. While Nbs1-CNS-ctrl oligodentrocytes developed processes that wrapped the axons of the optic nerve and determined the direction and organization of the myelin, Nbs1-CNS-Δ oligodentrocytes did not develop processes and lacked any trace of organization (Fig. 8, right panel). Similar to the optic nerve, retinal WT oligodentrocytes developed robust processes, while mutant oligodentrocytes lost their processes (Fig. 8, right panel). No differences in

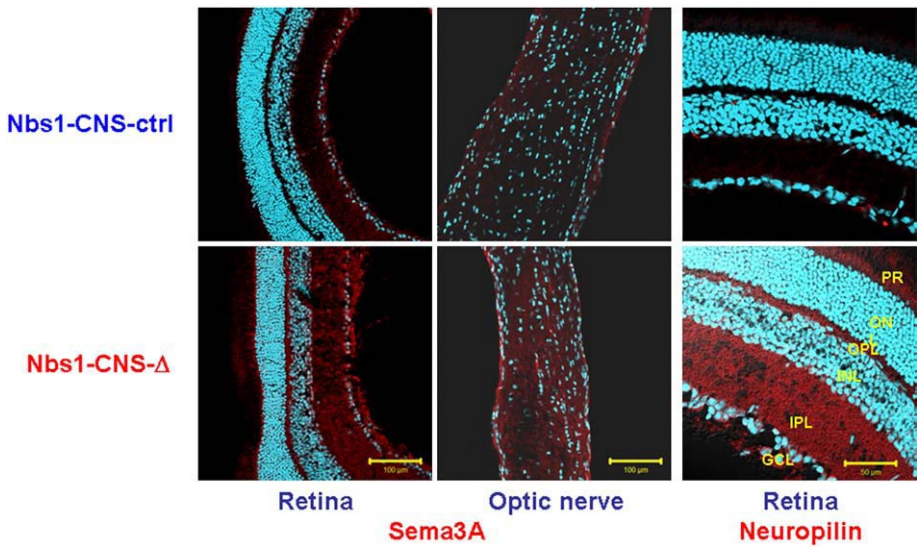

Fig. 7. Sema3A and NP1 up-regulation in Nbs1-CNS-Δ visual system. Nbs1-CNS-Δ and Nbs1-CNS-ctrl retinas and optic nerves were dissected at the age of 8–12 weeks and histological sections were subjected to immunohistochemistry either with anti-Sema3A or NP-1 antibodies. (Left panel), horizontal sections of retinas display Sema3A up-regulation in the Nbs1-CNS-Δ mice. (Middle panel), saggital sections of optic nerves display Sema3A up-regulated in the Nbs1-CNS-Δ mice. (Right panel), horizontal sections of retinas display NP-1 up-regulation in the Nbs1-CNS-Δ mice. These are representative photographs illustrating the results of three different mice from each of the Nbs1-CNS-Δ and Nbs1-CNS-ctrl genotypes.

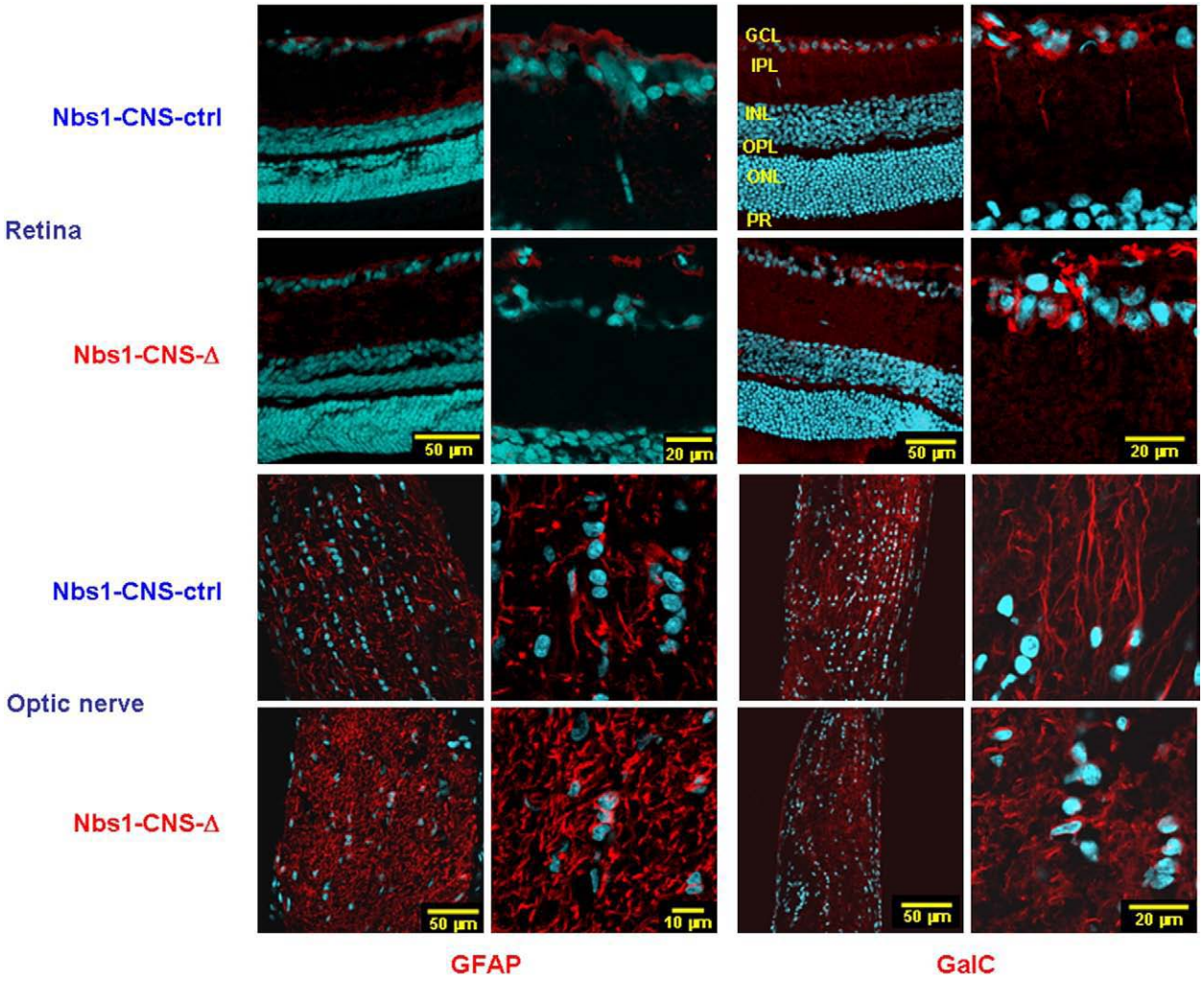

Fig. 8. The effect of Nbs1 deletion on Muller (astrocytes)- and microglial cells expression and organization. Nbs1-CNS-Δ and Nbs1-CNS-ctrl retinas and optic nerves were dissected at 8–12 weeks and histological sections were subjected to immunohistochemistry with anti-GFAP or anti-IB4 antibodies. (Left upper panel), horizontal sections of retinas of Nbs1-CNS-Δ mice displayed reduced expression of GFAP-expressing cells. (Left lower panel), saggital sections of optic nerve were immunoreacted with anti-GFAP antibody. Nbs-1 deletion led to an elevated number of GFAP-expressing cells in the optic nerve. (Right panel), whereas, the microglial cells in Nbs1-CNS-ctrl optic nerve assumed an organized structure with elongated and directed processes, no such organization was seen and loss of elongated and directed processes are evident in Nbs1-CNS-Δ optic nerve. These are representative photographs illustrating the results of three different mice from each of the Nbs1-CNS-Δ and Nbs1-CNS-ctrl genotypes (Sommer and Schachner, 1981).

oligodentrocyte morphology were observed between newborn WT and Nbs1-CNS-Δ retinas (Fig. S8). Collectively, our results demonstrate that Nbs1 loss seriously hampered the organization of glial cells in the optic nerve as well as in the retina.

Discussion

We found that conditional knock-out of Nbs1 in the CNS severely affects the visual system morphologically, biochemically and functionally. Reduction of Nbs1 levels in the retina caused loss of retinal functionality, evidenced by marked reduction in ERG amplitudes, axonal degeneration, demyelination and optic nerve disorganization. Nbs1 deletion leads to increased expression of the axonal guidance molecule Sema3A and its receptor NP-1, suggesting that Nbs1 loss induced a condition that resembles optic nerve injury (Nitzan et al., 2006). Conventional MRI markers (T_2) showed structural alterations in the lens, while the white matter-specific markers (FA, $D_\perp$) demonstrated significant damage to the white matter of the optic nerve.

T_2 is the most basic contrast mechanism in MRI. In the present study, T_2 increased significantly in the lens region of the mutant animals, associated with hyper-intense signal, strongly suggesting that the structure of the lens of these mice is impaired. T_2 does not, however, indicate the nature of the impairment. It is possible that the water content in the Nbs1-CNS-Δ lens is higher, or that the viscosity of the mutant lens is reduced — a state that increases the 3-dimensional motion of the water molecules. Indeed, the viscosity of isolated mutant lenses was markedly reduced, confirming the MRI observations. In contrast to the T_2 measures, DTI and its indices (FA, ADC and $D_\perp$) are more specific: they measure the translational motion of water molecules (Basser and Pierpaoli, 1998; Pierpaoli and Basser, 1996; Pierpaoli et al., 1996) and therefore give more details on white matter pathology. While ADC provides the averaged 3-dimensional diffusion coefficient and is not specific to gray or white matter, FA and $D_\perp$ provide unique information on white matter. FA measures the motional anisotropy of water molecules in the tissue: in white matter this anisotropy is high as the motion along the fibers is fast and perturbed perpendicular to them (Basser and Pierpaoli, 1998; Pierpaoli and Basser, 1996; Pierpaoli et al., 1996). Using DTI, it is possible to estimate the diffusion parallel and perpendicular to the fibers ($D_{||}$ and $D_\perp$), and the normalized differences between them. In most neurological disorders affecting the white matter, FA decreases and $D_\perp$ increases (Mori and Zhang, 2006; Neil et al., 2002; Sundgren et al., 2004), indicating either loss of fibers or demyelination, with no possibility to differentiate between the two processes. We also observed significant changes in these two parameters in the Nbs1-CNS-Δ mice that were indicative of white matter pathology of the

optic nerve. The histological findings presented in this study suggest that the MRI signal changes in the optic nerve do indeed originate from under-development and degeneration of this system (low number of axons, disorganization of the axons and poorly structured myelin. In an attempt to trace the origin of the white matter disorder we performed histological analyses of oligodentrocytes (Fig. 8). The oligodentrocytes in Nbs1-CNS-ctrl optic nerves are well organized; in the mutant genotype this organization is completely lost and the oligodentrocytes do not appear to produce ordered structure of myelin. These histological data was supported by electron microscopy findings of large axons with a small number of myelin wraps around them.

Nbs1 inactivation was also associated with elevated expression of the secreted neuro-repellent molecule Sema3A (Fig. 7). It has been shown that CNS induction of Sema3A expression in the adult was associated with neuronal injury and cell attrition (Charrier et al., 2003; De Winter et al., 2002; Nitzan et al., 2006; Shirvan et al., 2002). The fact that Sema3A up-regulation was not observed in newborn retinas but rather in adult retinas, suggest that conditional Nbs1 deletions lead to the formation of neurodegenerative disease. Nbs1 inactivation induced a state of neurodegeneration, which is interpreted by the visual system as injury, leading to increased expression of sema3A. The fact that the levels of phopho-p38 or JNK/phospho-Jun were not elevated suggests that classical apoptotic process is not involved in Nbs1 inactivation-induced neurodegeneration of the visual system. Further support for the notion that Nbs1 inactivation generates injury comes from the observation of astrogliosis in the mutant optic nerve (Fig. 8). In our previous study, we found that optic nerve injury was associated with astrocytosis (Nitzan et al., 2006). Collectively, our data support the notion that Nbs1 loss, which led to malfunction DDR, generates cell or tissue injury-like effects. Based on our previous studies, we assume that the injury-like conditions generated in response to Nbs1 loss are those that lead to the induction of Sema3A and NP1. However, we cannot exclude the possibility that defective activation of the DDR can directly induce the expression of the Sema3A-NP1 system. We are not aware at the present time of any link between DDR and the semaphorin-NP1 system.

Up-regulation of Sema3A in the adult CNS can activate apoptotic processes in certain cell populations (Gagliardini and Fankhauser, 1999; Shirvan et al., 2002; Shirvan et al., 1999). Since RGCs express Sema3A (de Winter et al., 2004), it is possible that Sema3A induction following Nbs1 inactivation plays a key role in the process that leads to RGC axonal degeneration in Nbs1-CNS-Δ retinas. For the Sema3A signaling to occur, it has to activate the NP-1 receptor complex, which was found to be expressed in the RGC (de Winter et al., 2004; Pasterkamp and Verhaagen, 2006). Activation of NP-1 is necessary to induce neuronal and axonal demise (Barr et al., 2005; Ochiumi et al., 2006; Shirvan et al., 1999). Concomitant induction of Sema3A and NP-1 in Nbs1-CNS-Δ mice supports the notion that these molecules are involved in axonal damage of RGCs.

Collectively, our data favor the possibility that conditional inactivation of Nbs1 does not severely affects retinal development, but rather leads to neurodegeneration. More severe changes are found in the optic nerve. Whereas at birth the organization of the mutant optic nerve appears similar to that of the Nbs1-CNS-ctrl, at age 2 months the mutant optic nerve displays severe disorganization as judged by the ECM morphology. Moreover, the adult mutant optic nerve displays a reduced number of axons, which lost their typical morphology and had undergone demyelination. These findings resemble acute optic nerve injury (Nitzan et al., 2006). Together, these findings raise an interesting possibility that defective DDR can initiate a neurodegenerative disease. In the visual system, malfunction in DDR leads to demyelination and axonal attrition. In our previous study we noticed that Nbs1 affects white matter integrity (Assaf et al., 2008). In addition to the optic nerve, Nbs1 deletion severely affects retinal functionality as measured by reduced ERG.

Interestingly, no signs of visual impairments were reported in NBS patients. This may be explained by the presence of truncated C-terminal Nbs1 proteins or hypomorphic mutations of this protein (Varon et al., 1998; Weemaes et al., 1981), which may sustain partial function of the MRN complex. Thus, visual system pathology in the mutant mice suggests that the hypomorphic mutations of Nbs1 may fail to reveal some of the essential functions of Nbs1 *in vivo*.

These data illustrate the importance of the DDR system for normal development, CNS organization, the long-term maintenance of the CNS and functionality of the nervous system.

Acknowledgments

The MRI scanner used in this study was purchased with a grant from The Israel Science Foundation. This work was supported by research grants from the A-T Children's Project, the Israel Science Foundation and the US-Israel Binational Science Foundation (to A.B.), and The A-T Medical Research Foundation, The A-T Children's Project, the A-T Medical Research Trust and the A-T Ease Foundation (to Y.S.). ZQW is supported by the Association for International Cancer Research (AICR) UK and Deutschen Forschungsgemeinschaft (DFG). A.B. Y,S, and ZQW were supported by the German-Israel Foundation (GIF).

Appendix A. Supplementary data

Supplementary data associated with this article can be found, in the online version, at doi:10.1016/j.expneurol.2009.03.026.

References

Assaf, Y., Galron, R., Shapira, I., Nitzan, A., Blumenfeld-Katzir, T., Solomon, A.S., Holdengreber, V., Wang, Z.Q., Shiloh, Y., Barzilai, A., 2008. MRI evidence of white matter damage in a mouse model of Nijmegen breakage syndrome. Exp. Neurol. 209, 181–191.

Barr, M.P., Byrne, A.M., Duffy, A.M., Condron, C.M., Devocelle, M., Harriott, P., Bouchier-Hayes, D.J., Harmey, J.H., 2005. A peptide corresponding to the neuropilin-1-binding site on VEGF(165) induces apoptosis of neuropilin-1-expressing breast tumour cells. Br. J. Cancer 92, 328–333.

Basser, P.J., Pierpaoli, C., 1998. A simplified method to measure the diffusion tensor from seven MR images. Magn. Reson. Med. 39, 928–934.

Carney, J.P., Maser, R.S., Olivares, H., Davis, E.M., Le Beau, M., Yates 3rd, J.R., Hays, L., Morgan, W.F., Petrini, J.H., 1998. The hMre11/hRad50 protein complex and Nijmegen breakage syndrome: linkage of double-strand break repair to the cellular DNA damage response. Cell 93, 477–486.

Charrier, E., Reibel, S., Rogemond, V., Aguera, M., Thomasset, N., Honnorat, J., 2003. Collapsin response mediator proteins (CRMPs): involvement in nervous system development and adult neurodegenerative disorders. Mol. Neurobiol. 28, 51–64.

Chrzanowska, K.H., Kleijer, W.J., Krajewska-Walasek, M., Bialecka, M., Gutkowska, A., Goryluk-Kozakiewicz, B., Michalkiewicz, J., Stachowski, J., Gregorek, H., Lyson-Wojciechowska, G., et al., 1995. Eleven Polish patients with microcephaly, immunodeficiency, and chromosomal instability: the Nijmegen breakage syndrome. Am. J. Med. Genet. 57, 462–471.

de Winter, F., Cui, Q., Symons, N., Verhaagen, J., Harvey, A.R., 2004. Expression of class-3 semaphorins and their receptors in the neonatal and adult rat retina. Invest. Ophthalmol. Vis. Sci. 45, 4554–4562.

De Winter, F., Holtmaat, A.J., Verhaagen, J., 2002. Neuropilin and class 3 semaphorins in nervous system regeneration. Adv. Exp. Med. Biol. 515, 115–139.

Digweed, M., Sperling, K., 2004. Nijmegen breakage syndrome: clinical manifestation of defective response to DNA double-strand breaks. DNA Repair (Amst) 3, 1207–1217.

Dumon-Jones, V., Frappart, P.O., Tong, W.M., Sajithlal, G., Hulla, W., Schmid, G., Herceg, Z., Digweed, M., Wang, Z.Q., 2003. Nbn heterozygosity renders mice susceptible to tumor formation and ionizing radiation-induced tumorigenesis. Cancer Res. 63, 7263–7269.

Frappart, P.O., Tong, W.M., Demuth, I., Radovanovic, I., Herceg, Z., Aguzzi, A., Digweed, M., Wang, Z.Q., 2005. An essential function for NBS1 in the prevention of ataxia and cerebellar defects. Nat. Med. 11, 538–544.

Gagliardini, V., Fankhauser, C., 1999. Semaphorin III can induce death in sensory neurons. Mol. Cell. Neurosci. 14, 301–316.

Kelbanov, O., Nitzan, A., Raz, D., Barzilai, A., Solomon, A.S., 2009. Upregulation of Semaphorin 3A and the associated biochemical and cellular events in a rat model of retinal detachment. Graefe Arch. Clin. Exp. Ophthalmol. 247 (1), 73–86 (Jan).

Lavin, M.F., 2007. ATM and the Mre11 complex combine to recognize and signal DNA double-strand breaks. Oncogene 26, 7749–7758.

Lazarov-Spiegler, O., Solomon, A.S., Schwartz, M., 1999. Link between optic nerve regrowth failure and macrophage stimulation in mammals. Vision Res. 39, 169–175.

Lukas, J., Bartek, J., 2004. Watching the DNA repair ensemble dance. Cell 118, 666–668.

Luo, Y., Shepherd, I., Li, J., Renzi, M.J., Chang, S., Raper, J.A., 1995. A family of molecules related to collapsin in the embryonic chick nervous system. Neuron 14, 1131–1140.
Messersmith, E.K., Leonardo, E.D., Shatz, C.J., Tessier-Lavigne, M., Goodman, C.S., Kolodkin, A.L., 1995. Semaphorin III can function as a selective chemorepellent to pattern sensory projections in the spinal cord. Neuron 14, 949–959.
Moreno-Herrero, F., de Jager, M., Dekker, N.H., Kanaar, R., Wyman, C., Dekker, C., 2005. Mesoscale conformational changes in the DNA-repair complex Rad50/Mre11/Nbs1 upon binding DNA. Nature 437, 440–443.
Mori, S., Zhang, J., 2006. Principles of diffusion tensor imaging and its applications to basic neuroscience research. Neuron 51, 527–539.
Neil, J., Miller, J., Mukherjee, P., Huppi, P.S., 2002. Diffusion tensor imaging of normal and injured developing human brain — a technical review. NMR Biomed. 15, 543–552.
Nitzan, A., Kermer, P., Shirvan, A., Bahr, M., Barzilai, A., Solomon, A.S., 2006. Examination of cellular and molecular events associated with optic nerve axotomy. Glia 54, 545–556.
Ochiumi, T., Kitadai, Y., Tanaka, S., Akagi, M., Yoshihara, M., Chayama, K., 2006. Neuropilin-1 is involved in regulation of apoptosis and migration of human colon cancer. Int. J. Oncol. 29, 105–116.
Pasterkamp, R.J., Verhaagen, J., 2006. Semaphorins in axon regeneration: developmental guidance molecules gone wrong? Philos. Trans. R. Soc. Lond. B. Biol. Sci. 361, 1499–1511.
Pierpaoli, C., Basser, P.J., 1996. Toward a quantitative assessment of diffusion anisotropy. Magn. Reson. Med. 36, 893–906.
Pierpaoli, C., Jezzard, P., Basser, P.J., Barnett, A., Di Chiro, G., 1996. Diffusion tensor MR imaging of the human brain. Radiology 201, 637–648.
Raper, J.A., 2000. Semaphorins and their receptors in vertebrates and invertebrates. Curr. Opin. Neurobiol. 10, 88–94.
Seemanova, E., Passarge, E., Beneskova, D., Houstek, J., Kasal, P., Sevcikova, M., 1985. Familial microcephaly with normal intelligence, immunodeficiency, and risk for lymphoreticular malignancies: a new autosomal recessive disorder. Am. J. Med. Genet. 20, 639–648.
Shirvan, A., Ziv, I., Fleminger, G., Shina, R., He, Z., Brudo, I., Melamed, E., Barzilai, A., 1999. Semaphorins as mediators of neuronal apoptosis. J. Neurochem. 73, 961–971.
Shirvan, A., Kimron, M., Holdengreber, V., Ziv, I., Ben-Shaul, Y., Melamed, S., Melamed, E., Barzilai, A., Solomon, A.S., 2002. Anti-semaphorin 3A antibodies rescue retinal ganglion cells from cell death following optic nerve axotomy. J. Biol. Chem. 277, 49799–49807.
Solomon, A.S., Kimron, M., Holdengreber, V., Nizan, A., Yaakobowicz, M., Harness, E., Smorodinsky, N.I., Shirvan, A., Barzilai, A., 2003. Up-regulation of semaphorin expression in retina of glaucomatous rabbits. Graefes Arch. Clin. Exp. Ophthalmol. 241, 673–681.
Sommer, I., Schachner, M., 1981. Monoclonal antibodies (O1 to O4) to oligodendrocyte cell surfaces: an immunocytological study in the central nervous system. Dev. Biol. 83, 311–327.
Stracker, T.H., Theunissen, J.W., Morales, M., Petrini, J.H., 2004. The Mre11 complex and the metabolism of chromosome breaks: the importance of communicating and holding things together. DNA Repair (Amst) 3, 845–854.
Sundgren, P.C., Dong, Q., Gomez-Hassan, D., Mukherji, S.K., Maly, P., Welsh, R., 2004. Diffusion tensor imaging of the brain: review of clinical applications. Neuroradiology 46, 339–350.
van der Burgt, I., Chrzanowska, K.H., Smeets, D., Weemaes, C., 1996. Nijmegen breakage syndrome. J. Med. Genet. 33, 153–156.
Van Vactor, D.V., Lorenz, L.J., 1999. Neural development: the semantics of axon guidance. Curr. Biol. 9, R201–R204.
Varon, R., Vissinga, C., Platzer, M., Cerosaletti, K.M., Chrzanowska, K.H., Saar, K., Beckmann, G., Seemanova, E., Cooper, P.R., Nowak, N.J., Stumm, M., Weemaes, C.M., Gatti, R.A., Wilson, R.K., Digweed, M., Rosenthal, A., Sperling, K., Concannon, P., Reis, A., 1998. Nibrin, a novel DNA double-strand break repair protein, is mutated in Nijmegen breakage syndrome. Cell 93, 467–476.
Weemaes, C.M., Hustinx, T.W., Scheres, J.M., van Munster, P.J., Bakkeren, J.A., Taalman, R.D., 1981. A new chromosomal instability disorder: the Nijmegen breakage syndrome. Acta Paediatr. Scand. 70, 557–564.
Yang, Y.G., Frappart, P.O., Frappart, L., Wang, Z.Q., Tong, W.M., 2006. A novel function of DNA repair molecule Nbs1 in terminal differentiation of the lens fibre cells and cataractogenesis. DNA Repair (Amst) 5, 885–893.
Zhu, J., Petersen, S., Tessarollo, L., Nussenzweig, A., 2001. Targeted disruption of the Nijmegen breakage syndrome gene NBS1 leads to early embryonic lethality in mice. Curr. Biol. 11, 105–109.